J. Fluid Mech. (1992), *vol.* 245, *pp.* 619–641

Modifying turbulent structure with drag-reducing polymer additives in turbulent channel flows

By T. WEI[1] AND W. W. WILLMARTH[2]

[1] Department of Mechanical and Aerospace Engineering, Rutgers University, Piscataway, NJ 08855-0909, USA

[2] Department of Aerospace Engineering, University of Michigan, Ann Arbor, MI 48109-2140, USA

(Received 1 January 1991 and in revised form 13 May 1992)

New power spectra computed from LDA measurements of the fluctuating u- and v-velocity signals in a turbulent channel flow with and without drag-reducing polymer (polyethylene oxide) injection are presented. LDA data rates were sufficiently high to reconstruct the simultaneous time-dependent u- and v-velocity signals along with the time-dependent Reynolds stress signal. Time-averaged statistics of the turbulent flow are presented in conjunction with the power spectral measurements which show a dramatic reduction in both the v-velocity fluctuations and Reynolds stress fluctuations throughout the channel over all frequencies. There is also a redistribution of energy in the u-velocity fluctuations from high frequencies to low frequencies throughout the channel. Different injection conditions were examined; different polymer concentrations were injected at different flow rates such that the total amount of polymer in the channel remained constant. For certain polymer concentrations, 'large' negative Reynolds stress, $-\langle uv\rangle/u_\tau^2 \approx -0.2$, was measured in the near-wall region. In addition, there is a marked difference in the u-velocity spectra and the Reynolds stress spectra close to the wall for the different injection conditions.

1. Introduction

This paper is a report of new high-resolution measurements made in turbulent channel flows with drag-reducing polymer additives. The unique feature of the data presented in this report is the inclusion of power spectra for the fluctuating v-velocity and Reynolds stress signals. Time-averaged statistics of the turbulent fluctuating velocities are presented along with the new power spectra.

The polymer drag-reduction literature can be roughly divided into three categories. The first category includes works on drag reduction from a molecular perspective. The authors of these studies examine the behaviour of polymer molecules in various model flows (e.g. simple shear, pure strain, etc.) and extrapolate their findings to the fully turbulent case. One of the most recent examples of this type of work is the two-part paper by McCormick *et al.* (1990*a*, *b*).

The second category includes studies on the effects of polymers on the time-averaged turbulence statistics. This category includes much of the earliest work on polymer drag reduction. One of the best examples of this type of research was done by Virk *et al.* (1967). They measured mean velocity profiles with different molecular weight polymers dissolved in various solvents. Their work led to much of the earliest understanding of the significant variables in drag-reducing flows.

With advances in instrumentation and visualization techniques, a third category arose in which changes in coherent turbulent structure due to polymers are examined. Early LDA measurements in polymer drag-reducing flows were reported by Rudd (1972) and Reischman & Tiederman (1975). These single-component measurements were followed by the comparable studies of Berner & Scrivener (1979) and Berman (1986), which included power spectra of the fluctuating u-velocity that demonstrated a redistribution of energy from high frequencies to low frequencies close to the wall. Two-component LDA measurements were reported by Durst, Keck & Kline (1985), Willmarth, Wei & Lee (1987) and Luchik & Tiederman (1988). None of these works included spectra of either u or v. In other investigations, flow visualization studies and conditional sampling of turbulence velocity measurements have been used to study the effects of polymers on streak spacing, bursting frequency, and Reynolds stress production.

There are noteworthy papers from each of these categories which provide valuable insight into polymer drag reduction, yet there still is no clear picture of why or how polymers reduce drag. What appears to be lacking is a drag-reduction model which incorporates information from all three categories, from polymer molecule considerations, mean statistical measurements, and turbulent structure studies. To begin the bridging process across the three categories, a brief review of the literature from each is presented in the following paragraphs.

1.1. *The molecular approach*

One of the most thorough literature reviews of the dynamics of polymer molecules in turbulent flows was written by Lumley (1969). He enumerated a number of important molecular parameters including molecular weight, flexibility, length, expansion, filament formation. He reported a consensus opinion that drag-reducing polymer molecules in turbulent boundary layers are stretched by the flow, resulting in an increase in the local fluid viscosity. This hypothesis was later reiterated by Hinch (1977), and others.

Hinch (1977) used physical arguments in conjunction with existing polymer elongation models to hypothesize a drag-reduction mechanism. He proposed that the elongation of a long-chain polymer molecule results in a dramatic increase in the viscosity of the fluid in the immediate vicinity of the molecule. The more the molecule stretches, the greater the increase in local viscosity. He concluded that the degree to which a molecule will elongate depends on the strain rate of the fluid surrounding the polymer.

Zakin & Hunston (1980) emphasized the need for a 'good' solvent (i.e. one in which polymer–solvent interactions are dominant over polymer–polymer interactions). They further expounded on the importance of molecular relaxation time in drag reduction. Specifically, they pointed out that, in order to achieve drag reduction, the relaxation time of a stretched polymer molecule must be greater than the timescale of the flow. Berman (1977) agrees with this point. He showed that the critical onset shear rate is proportional to the viscous frequency, u_τ^2/ν.

A very recent theoretical study was conducted by Rabin & Zielinska (1989). They examined the effect of polymer molecules on the vorticity distribution in elongational flows. They began by pointing out that as long as the flow is Newtonian, vortex stretching occurs over all wavenumbers. Their analysis showed that the addition of polymers inhibits the stretching of vorticity at high wavenumbers. Energy that would have been dissipated by small-scale vortices is transferred to and stored in the extended polymer molecules. When the molecules advect into regions of low strain

rate, they relax back into the natural state of a tangled ball. In so doing, the stored energy is returned to the low-wavenumber velocity fluctuations. Thus, Rabin & Zielinska (1989) argued, there will be a shift in the turbulent energy from high down to low wavenumbers.

The shortcoming of a purely molecular approach is that it is difficult to rigorously extend the analysis to turbulent wall-bounded flows. This is primarily due to the complexity of the boundary layer. Thus, Hinch (1977), Rabin & Zielinska (1989), and others were not able to specifically identify regions of the flow where the stretching of polymer molecules would most likely lead to drag reduction.

1.2. *Turbulence statistics measurements*

Among the most careful and extensive of the early velocity studies of drag-reducing flows is the work by Virk *et al.* (1967). They used both Pitot probes and hot-film anemometry to measure the streamwise velocity in a drag-reducing pipe flow with a number of drag-reducing polymers and different solvents. This work produced the well known 'Virk asymptote' for drag reduction as a function of polymer concentration.

More recently, the issue of homogeneous versus non-homogeneous drag reduction has arisen. It has been observed by a number of researchers that the amount of drag reduction depends greatly on whether the polymer is pre-mixed or injected into a Newtonian flow. Stenberg *et al.* (1977), McComb & Rabie (1982), and Berman (1986) all studied this problem. The feature of interest in non-homogeneous polymer solutions is the formation of filaments or threads. This is described by Lumley (1969) as an increase in the extensional viscosity of the fluid by the addition of polymers. Stenberg *et al.* (1977) observed that 'threads formed by the injected 0.2% suspension dissolved more readily than those of the 1% concentration' and that 'the impression was that very thin strands of additive were being peeled off continuously from the polymer string'. This work, and the pipe experiment of Bewersdorff (1984) have led to the thread hypothesis of drag reduction; drag reduction results through the interaction of polymer threads with the near-wall turbulent structure.

Unfortunately, mean measurements alone are insufficient for the study of turbulent structure. In addition, the early measurements were hampered by experimental difficulties in measuring velocities with an intrusive measuring device. For example, polymer molecules wrap themselves around hot-film sensors which drastically changes the heat transfer characteristics of the sensor. The development of the LDA solved the intrusive probe problem. This led to measurements with greater accuracy and resolution which could be used to study the coherent near-wall structure.

1.3. *Polymer effects on turbulent structure*

Drag-reduction research received new impetus from the coherent turbulent boundary layer structure research initiated by Kline *et al.* (1967). One of the first papers addressing the effect of polymers on coherent structure was written by Gordon (1970). He proposed that drag-reducing polymers cause a reduction in the intensity of the burst. However, he produced no data to support this hypothesis.

Donohue, Tiederman & Reischman (1972) employed food colour dye flow visualization to examine the effects of polymers on turbulent coherent structure. They conducted experiments in a turbulent channel flow with polyethylene oxide. They reported a dramatic attenuation of the y-fluid motions close to the wall, and an increase in the streak spacing and a significant decrease in the bursting rate.

Achia & Thompson (1977) used real-time holography to visually examine the

turbulent near-wall structure in a circular pipe. They reported that the addition of Separan caused a suppression of the burst process and a concomitant increase in streak spacing. Berman (1986) also reported a decrease in the bursting rate with the addition of polymers. He reported the greatest reduction in burst frequency for injected polymers. Berman (1986) further found that premixed polymers also reduce the bursting rate but not as well as in the injection case.

More recent works by Tiederman, Luchik & Bogard (1985) and Luchik & Tiederman (1988) have begun to focus on the fine structure of the bursting process. Burst detection algorithms were employed on turbulent channel flow data with and without the addition of Separan. It was reported that the polymer did not affect the general shape of the conditionally sampled burst signals. However, there was a reduction in the bursting rate and an increase in streak spacing. This last observation was consistent with earlier studies from Tiederman's laboratory.

The problem with the coherent structure research is the inability to explain why the bursting frequency decreased and the streak spacing increased. Such an explanation would probably require an understanding of polymer molecular dynamics. Thus, there are two questions to be answered. How are polymer molecules influenced by the near-wall turbulent structure? And, second, how do the molecules, in turn, alter the near-wall turbulence?

These are difficult questions indeed. One must first identify the regions in the flow where the polymers are when drag reduction occurs, how the polymer molecules are distributed throughout these regions, and what the dynamically important turbulent structures are in those polymer-filled regions. One then can one begin to understand how the polymer molecules interact with the turbulence.

As a first step in this process, a study of a turbulent channel flow with polymer injection was studied. Three different concentrations of polyethylene-oxide were injected into the channel at different injection rates so that the total amount of polymer in the channel was the same. The results of this study would provide information about where the polymer most significantly affected the turbulent structure, and whether different injection concentrations affect the distribution of polymer molecules in the flow.

2. Apparatus

2.1. *Turbulent channel flow facility*

Experiments were conducted in the closed-circuit turbulent channel flow facility described in Wei & Willmarth (1989). A schematic diagram of the experiment appears in figure 1. The only significant change since then was the addition of a polymer injection system; this will be described in §2.2. The channel test section dimensions were 345.44 cm in length, 2.572 cm in width, and 30.48 cm in height. These dimensions correspond to the x-, y-, and z-directions, respectively. The measurement station was located 223.52 cm downstream of the test section inlet. An LDA measurement volume was created by the intersection of four laser beams as shown in figure 2. The beams were oriented so that two-component measurements were made along the principal axes of the flow, i.e. 45° into the wall and 45° away from the wall. Each laser beam was focused to a waist at the measurement volume, and the light scattered from the measurement volume was observed in sidescatter. In this manner, the spatial resolution of the LDA measurements was approximately 50 μm. The reader is referred to Wei & Willmarth (1989) or Wei (1987) for specific details of the experiment.

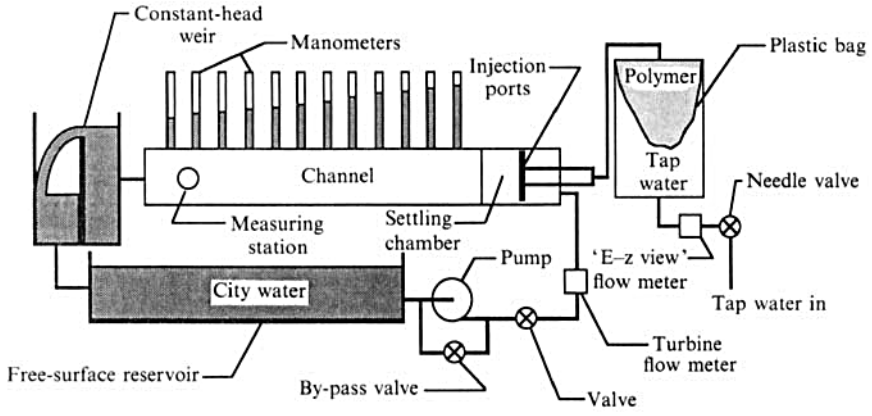

FIGURE 1. Schematic drawing of the water channel facility including the polymer-injection system.

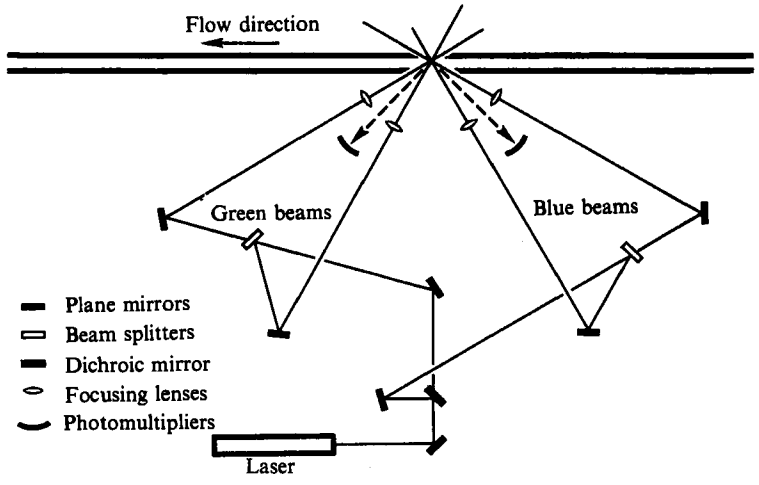

FIGURE 2. Top-view schematic drawing of the laser beam paths. Note that the beams angles/orientations are correct. However, the lengths are not to scale.

2.2. *Polymer injection system*

A polymer injection system was designed to supply a steady flow of concentrated polymer solution to the channel without degrading the polymer in the process. The polymer used in this study was polyethylene oxide (PEO) (Polyox WSR-301). A schematic diagram of the injection system is shown in figure 3. It is a positive displacement system in which polymer is displaced from the supply tank by a steady flow of tap water.

The supply tank was a 200 l steel drum. The bottom of the drum was connected by a pipe to the city water supply. A flow of water into the drum could be regulated with a needle valve and monitored using an in-line, positive-displacement flow meter. The drum had a removable cover which was clamped in place during the experiment. A flexible pipe connected the drum from its top to the channel settling chamber, as shown in figure 3.

To inject polymers into the channel, the drum was first lined with a 200 l plastic bag. The bag was then filled with a solution of PEO of known concentration. The drum cover was subsequently tightly clamped in place (the cover was supplied with

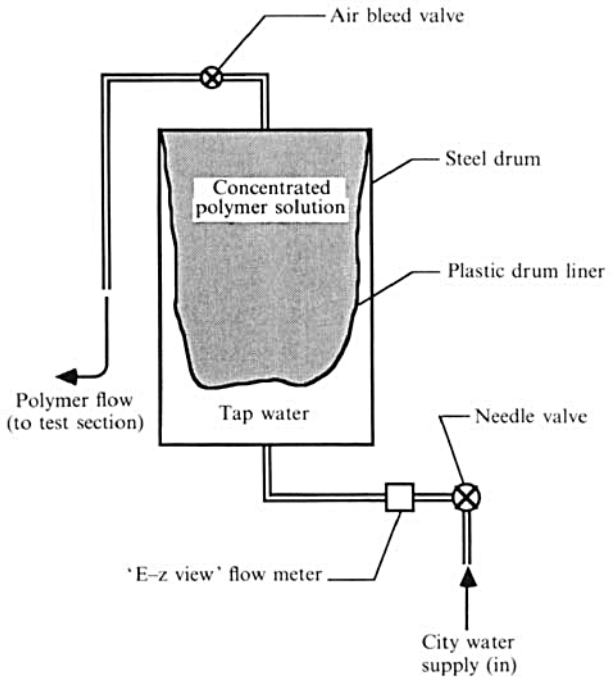

FIGURE 3. Schematic drawing of the polymer-injection system.

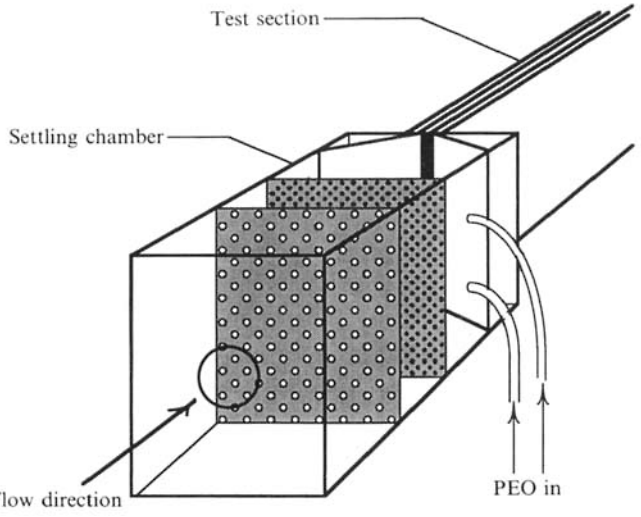

FIGURE 4. Oblique-view sketch of the settling chamber. Flow is obliquely into the page. The shaded grey rectangles represent the turbulence damping screens.

a rim seal which prevented leakage). By opening the needle valve at the bottom of the drum, a flow of tap water entered the drum beneath the plastic bag. This forced polymer out of the top of the drum at the same flow rate as the incoming tap water. In this manner, a supply of polymer could be injected into the channel at a constant flow rate without degrading the polymer.

Figure 4 is an oblique-view drawing showing how the polymer injection lines were connected to the settling chamber. The settling chamber was a rectangular Plexiglas box with outside dimensions of 30.48 cm in width, 38.10 cm in height, and 64.77 cm

in length. Flow entered the settling chamber through a 10.16 cm pipe centred on the upstream face. Two stainless steel perforated plates were placed inside the settling chamber to break up the large eddies generated at the inlet. The first screen, with 0.635 cm diameter holes, was 21.59 cm downstream of the settling chamber inlet. The second plate, with 0.159 cm diameter holes, was located 12.7 cm downstream of the first. The holes in the plate were arranged in a hexagonal pattern with spacing such that the ratio of open area to total area was approximately 0.4. The mean flow speed in the settling chamber was 6.45 cm/s.

The settling chamber was designed to provide a region in which the flow was turbulent but without large eddies so that the injected polymer could be uniformly mixed before the flow entered the channel. The perforated plates served to break up eddies with scale of the order of the inlet pipe diameter or larger while producing smaller scale turbulence with a slow rate of decay. Bradshaw (1965) showed that effective damping of small-scale turbulence by screens required that the ratio of open area to total area should be greater than ≈ 0.57. He further showed that, for screens with smaller area ratios, jets of fluid emanating from adjacent openings tend to coagulate and produce larger eddies which decay at a slower rate.

Polymer injection lines were connected to the settling chamber 8.5 cm downstream of both plates. This was done to prevent polymer degradation by the plates. The 2.54 cm diameter polymer injection line from the 200 l supply tank was divided into four 1.27 cm diameter lines using a two stage 'tee' arrangement. Hence, there were four injection lines entering the settling chamber, two on each side. The lower line of each pair was placed 12.7 cm above the floor of the settling chamber and the upper lines were connected 25.4 cm above the floor, as shown in figure 4.

Approximately 8 cm downstream of the polymer injection ports, the flow passed through a two-dimensional plane-walled contraction section. This linearly reduced the width of the flow from 30.48 cm to 2.54 cm in a distance of 14 cm. There is strong evidence showing that the polymer was distributed throughout the flow upstream of the channel. A discussion of the effectiveness of the polymer injection system in the context of mixing appears in §3.1.

3. Experimental conditions

Data are presented from four separate experimental runs where the master solution concentration and the polymer injection rate were varied. In all four cases the water flow rate in the channel was 360 l/min. The first case was the Newtonian baseline case, during which no polymer was injected. In the three polymer runs, master solution concentrations of 500, 1000, and 2000 p.p.m. by weight of PEO were tested. In each case, the master solution was injected so that the homogeneous concentration in the channel would be 10 p.p.m. That is, the 500 p.p.m. master solution was injected at a rate of 7.2 l/min (resulting in a 50:1 dilution of the master solution), the 1000 p.p.m. master solution at 3.6 l/min, and the 2000 p.p.m. master solution at 1.8 l/min. Note that some of the data for the Newtonian and the 1000 p.p.m. PEO cases were presented in Willmarth *et al.* (1987). Table 1 lists the significant flow parameters for each of the four cases. The Reynolds number in all four cases was approximately 12000, based on the centreline velocity, and, b the half-channel width.

In the three polymer runs, the following procedure was followed. First, a 360 l/min flow of water was established in the channel. A number of LDA measurements in water were made both close to the wall and close to the channel centreline. These

Plotter symbol	Master solution concentration (p.p.m.)	Injection rate (l/min.)	'Homogeneous' concentration (p.p.m.)	Re	u_τ (cm/s)	% Drag reduction
+	0	—	0	12182	4.50	—
○	500	7.2	10	11776	3.86	30%
□	1000	3.6	10	12628	3.80	32%
△	2000	1.8	10	11937	3.59	39%

TABLE 1. Significant flow parameters for the Newtonian and drag-reducing flows. Plotter symbols appear in the first column and are consistently used in all of the following plots.

data were later used to determine the wall location by computing the average streamwise velocities and fitting those values to the mean profile compiled by Coles (1953). A flow of PEO was then initiated from the supply drum at the desired flow rate. A minimum of five minutes was allowed to elapse in order to ensure that the pressure gradient in the channel had stabilized to its new value. After equilibrium was established, LDA data in the drag-reducing flow were acquired.

For each of the four runs, the LDA data rates were sufficiently high that it was possible to reconstruct the time-dependent u- and v-velocity signals. Again, a detailed discussion may be found in Wei & Willmarth (1989). The u- and v-traces were reconstructed at even time intervals and digitally filtered with a Gaussian window. In this way, time averages could be obtained by simply ensemble averaging the reconstructed signals. Sufficiently long data records were obtained in order to assure accurate time averages.

3.1. *Notes on the completeness of polymer mixing in the settling chamber*

The usefulness of the present results to future studies on drag reduction depends heavily on how well the injected master polymer solution mixed with the main flow of solvent. If the polymer did not mix rapidly after injection, the data would exhibit trends which were injection-geometry dependent. For example, one might argue that the injected polymer solution formed four 'ropes', one from each injection port, which extended far into the channel. Filaments of polymer, or 'threads', would peel away from the main 'ropes' as the 'ropes' meandered along the channel. One would imagine that the 'ropes' would eventually break up through this peeling away process. Clearly, 'ropes' formed from lower-concentration polymer solutions would break apart more rapidly than higher-concentration 'ropes'. And thus, the injection system would produce different flows for different injection concentrations.

In this section, it will be argued that the four injection polymer 'ropes' broke up into fine filaments before the flow entered the channel. That is, because of the injection geometry and injection concentrations, polymer threads were uniformly distributed throughout the flow very quickly. It is recognized that it is difficult to rigorously quantify the mixing of the injected polymer solution with the solvent. However, a number of arguments will be developed which support the claim that the polymers were thoroughly distributed in the flow. These include discussions of polymer thread formation taken from the literature, visual observations of the polymer injection, and a simple, but enlightening, model of the effects of 'ropes' on the pressure gradient in the channel.

A strong argument supporting the rapid distribution of polymers in the flow may be developed from the literature on polymer injection in pipe flows. Recent work by Usui (1990) and Berman (1990) and an earlier study by Stenberg *et al.* (1977) on the

nature of mixing of concentrated polymer with a solvent provide a qualitative description of the fluid in the channel. All three of these references were investigations of single concentrated polymer threads injected in the centre of a fully developed turbulent pipe flow. The range of thread concentration across the three works was < 500 to 10000 p.p.m. Usui (1990) visually observed PEO threads marked with coloured dye. He noted that for thread concentrations below 500 p.p.m. the injected thread immediately dispersed throughout the pipe. Owing to his visualization technique, he was not able to determine how the polymer was distributed. He further observed that a thread with an 'intermediate' concentration in the range 2000 to 4000 p.p.m. would break up into a large number of fine threads. This was independently confirmed by Stenberg *et al.* (1977) and Berman (1990). Stenberg *et al.* (1977) observed that some of the polymer in a 2000 p.p.m. thread moved away from the thread as dilute polymer solution. They described this as a peeling away of layers of polymer from the thread. Berman's (1990) work indicates that the breakup into fine threads and subsequent peeling away of polymers from the fine threads occurs for injection concentrations as high as 6000 p.p.m. For concentrations greater than 8000 p.p.m. there is a consensus amongst the three works that the injected thread remains intact.

In a private discussion in 1991, N. S. Berman pointed out that the behaviour of drag-reducing polymers depends very heavily on how old the polymer is. He noted that the critical parameter for determining the age of a polymer sample is the intrinsic viscosity, η, of the polymer solution:

$$\eta = c_{\text{polymer}}^{-1}\{(\nu_{\text{polymer}}/\nu_{\text{solvent}}) - 1\}, \tag{1}$$

where c_{polymer} is the polymer concentration in g/dl, and ν_{polymer} and ν_{solvent} are the kinematic viscosity of the polymer solution and the solvent (i.e. water), respectively. Berman stated that the intrinsic viscosity of a polymer sample decreases with the age of the polymer. In his studies, the intrinsic viscosity of his polymers were less than 10 dl/g. A new PEO sample would have values of η approximately equal to 20 dl/g. He pointed out that comparisons between polymer studies could only be carried out if the intrinsic viscosities of the polymer solutions were similar.

The PEO used in this study came from a sample which was purchased nearly twenty years ago. Therefore, it is highly likely that the polymer could be considered to be 'old'. To test this hypothesis, the intrinsic viscosity of a 100 p.p.m. (0.01 g/dl) PEO solution was measured using a no. 50 Cannon-Fenske routine viscometer. For the PEO used in the present study, η was found to be ≈ 8.5 dl/g which compares quite well with the value quoted by Berman (1991, private communication). Therefore, it is argued that the observations reported in the literature, particularly those by Berman (1990), are valid for the polymers used in the present investigation.

In this study, the range of injected polymer concentration was comparatively low, from 500 to 2000 p.p.m. Based purely on the observations of the behaviour of injected polymer solutions described by Berman (1990) and Usui (1990), it is likely that the injected polymer rapidly dispersed immediately after injection. Usui (1990) reported that the fine polymer threads which were created by the breakup of the injected polymer thread were advected by the large-scale motions of the turbulent pipe flow. Photographs in that work clearly illustrate how quickly and uniformly the fine threads became distributed throughout the pipe. By extension, the fluid entering the channel, in the present study, was probably a homogeneous mixture of fine polymer threads, localized regions of water with no polymer, and small regions of dilute polymer solution which was not in thread form.

This was verified by conducting an experiment in which the PEO was mixed in a solution of fluorescein dye. As the dyed PEO solution was injected into the settling chamber, a third photomultiplier was used to detect the intensity of fluorescent light from the dyed polymer and thereby indicate the amount of dyed polymer solution passing through the LDA measuring volume. If the polymers were uniformly mixed in the channel, there would have been no fluctuations in the intensity of the fluorescent light from the dyed fluid passing through the measuring volume. This was not the case, however; there were relatively large fluctuations in the photomultiplier signal measuring the intensity of the fluorescent light. It was not possible to distinguish between the passage of a fine polymer thread and a region of dilute polymer. However, the experiment clearly showed temporal variations in the polymer concentration in the channel.

The breakup of the injected polymer 'ropes' was further enhanced because of two features designed into the injection system. First, as described in §2.2, the flow in the settling chamber passed through two stainless steel perforated plates. The plates broke up the large scales from the upstream inlet pipe but ensured that the flow remained turbulent; the flow in the settling chamber was, by design, highly turbulent even downstream of the plates. This background turbulence acted to mix the polymer upon injection into the settling chamber.

Second, the injection speeds were sufficiently high to promote mixing in the settling chamber. Again, as stated in §2.2, the mean flow speed in the settling chamber was 6.45 cm/s. By comparison, the speed of the injected polymer in the 1.27 cm diameter lines was approximately 24, 12 and 6 cm/s for injected polymer concentrations of 500, 1000, and 2000 p.p.m. respectively. Thus, the speed of the injected polymer solution was greater than or equal to the flow speed of the water in the setting chamber. Since the polymer was injected perpendicular to the mean flow in the settling chamber at a relatively high speed, it is clear that a significant amount of mixing would occur close to the injection point. This is in contrast to other injection studies where polymers are generally injected in the flow direction at the local mean speed. It is therefore reasonable to assume that the turbulent motions in the present flow in the settling chamber and contraction section would rapidly distribute the polymer throughout the flow upstream of the channel. So, while there would be local variations in polymer concentration, the mean polymer concentration throughout the channel was believed to be uniform.

Further evidence of the polymer mixing in the settling chamber was obtained from visual observations of the settling chamber flow made during the fluorescein dye concentration measurement experiments. It was observed at that time that the four jets of injected polymer/fluorescein solution, which were moving more rapidly than the settling chamber flow speed, caused considerable mixing. The dyed polymer solution was observed everywhere in the cross-section of the settling chamber downstream of the perforated plates and in the contraction section.

The final and perhaps strongest supporting argument for rapid and thorough distribution of the polymers in the settling chamber was the linearity of the pressure gradient in the channel. As described in Wei (1987) and Wei & Willmarth (1989), the pressure gradient in the channel was monitored using a set of 15 large-diameter (3.8 cm) glass tube manometers spaced 15.24 cm apart. The large diameter of the manometers served to average the pressure fluctuations and reduce measurement errors caused by the tendency of the meniscus to stick to the walls of the manometer tube. In all cases, the pressure gradient in the channel with or without polymer injection was linear from the first to the last manometer, located 24.13 and 237.49 cm

downstream of the channel inlet, respectively. (The measuring station was 223.52 cm downstream of the channel inlet.)

The linearity of the pressure gradient was checked throughout each run for each polymer concentration by observing the height of the fluid in each manometer tube and visually comparing the fluid level in each of the 15 manometers to a sloping line provided by two mono-filament fishing lines stretched along either side of the manometer tubes. The use of two lines ensured that parallax error was avoided. The height of the monofilament lines was adjusted and measured using two vertical precision traverse slides at either end of the lines. The lines were positioned to match the height of the fluid in the first and last manometer at the beginning of each run. It was found, by visually comparing the height of the fluid in a manometer tube to the height of the monofilament lines, that the pressure at any particular manometer could be determined to within 0.5 mm of water. As previously stated, the pressure gradient was constant along the channel for all the runs with polymer or water. Since the difference in height of the fluid in the first and last manometer was approximately 2.25 cm for the flow with the largest drag reduction and 3.15 cm for water with no drag reduction, the pressure gradient was constant to within $\leqslant 3\%$ all along the channel for any run.

Now if one were to assume (incorrectly) that the polymer was not well distributed before entering the channel, this should become evident upon examination of the pressure gradient. That is, if spanwise mixing of the polymer in the channel was not complete, then the amount of drag reduction should vary as a function of distance downstream of the channel entrance. This, in turn, would result in a variation in the pressure gradient along the length of the channel. The pressure gradient will become constant only when the spanwise mixing is complete.

An estimate can be made of the variation in pressure and pressure gradient which might be caused by spanwise non-uniformity of the polymer. Let α be the pressure gradient for a fully developed channel flow of the solvent without polymer. Similarly, define β as the pressure gradient for a fully developed flow of a uniform mixture of polymer and solvent, with α and β less than zero.

Now assume that incomplete mixing across the span of the channel begins at some station $x = 0$, and results in a region containing both polymer and solvent. Note that this is a simple model of an injected polymer 'rope' in the channel from which fine 'threads' are being peeled away. Further assume that this polymer-containing region is wedge shaped as it grows linearly with distance downstream to the maximum width of the channel, W, in a distance, $x = L$. Outside the wedge, the fluid is pure solvent. The local width, $w(x)$, of the wedge-shaped region is given by

$$w(x) = Wx/L. \tag{2}$$

Because only the wedge-shaped region contains polymer, the reduction in pressure gradient at any station associated with the polymer is proportional to the width of the wedge. Further assume that the proportionality constant does not vary with distance downstream. Then the average pressure gradient at any station is average of the sum of the products of the width and pressure gradient for the solvent and for the wedge-shaped mixture of polymer and solvent. This gives the expression

$$\partial P/\partial x = [\alpha(W-w)+\beta w]/W = \alpha+(\beta-\alpha)\,x/L \tag{3}$$

for the pressure gradient at a distance x from the beginning of the mixing. By integrating (3), and substituting $x = L$, the pressure change at the end of mixing is

$$P-P_1 = \tfrac{1}{2}L(\alpha+\beta); \quad \alpha,\beta < 0, \tag{4}$$

where P_1 is the initial pressure at $x = 0$. The pressure change at the end of spanwise mixing in the channel would be readily observable; it is the average of the pressure change for no mixing, αL, and for complete mixing, βL. In spite of the simplicity of the assumptions in the above calculations, namely the assumed constant pressure gradient in the still-mixing polymer across the width of the channel in the equations above, the fact that no appreciable variation (greater than 3%) in the pressure gradient from linearity was observed in any of the runs with polymer addition supports the conclusion that the mixing was complete before the fluid reached the first manometer, 24.13 cm downstream of the channel inlet and $\approx$ 200 cm upstream of the measuring station.

Taken *in toto*, the polymer-injection geometry used in this study was not as irreconcilably different from other injection geometries (e.g. Tiederman's method of injecting polymers through a spanwise slot in the channel) as it may first appear. For the relatively low injection concentrations used in this investigation, Usui (1990) showed that the injected polymer would have rapidly dispersed, either as a dilute cloud, for the 500 p.p.m. case, or as a number of fine threads, in the 1000 and 2000 p.p.m. cases. The polymer was dispersed across the span of the channel by the turbulent motions in the settling chamber and contraction section so that, even at the station 24.13 cm downstream of the channel inlet, the average concentration of the polymer was constant across the span of the channel. This, as discussed above, was supported by the linearity of the pressure gradient beginning with the first manometer in the channel. When the mixture of water and injected polymer passed through the measurement station, the fine threads, regions of dilute polymer, and regions of solvent were well distributed across the cross-section of the channel. Therefore, it is argued that the present data are virtually independent of injection geometry; they should be comparable with other studies of drag reduction by uniform polymer injection. This might not have been true had much higher injection concentrations been tested.

It will be convenient to define the term 'homogeneous concentration' as the concentration of polymer in the channel that would have been achieved if the polymer had become thoroughly mixed to a uniform concentration after injection. The 'master solution concentration' will denote the polymer concentration in the 200 l supply tank prior to injection. The recirculation pump was instrumental in preventing the buildup of polymer in the flow loop. Owing to the high shear rates in the pump, the polymer molecules degraded as they passed through the pump, thereby losing their drag-reducing properties. Again, the pressure gradient measurements provided proof that the polymer concentration in the channel remained constant. If the polymers were not completely degraded by the pump, then the concentration of drag-reducing polymers in the flow loop would increase with time as fresh polymer was continuously being injected into the loop. Were that the case, it would be expected that the amount of drag reduction would also increase with time. This could be visually observed by a steady decrease in the pressure gradient. In fact, the pressure gradient remained constant throughout the duration of every run. Therefore, it was concluded that the average concentration of drag-reducing polymers in the channel remained constant.

3.2. *A note on seeding-particle injection*

It should be noted that LDA seeding particles were injected into the settling chamber through a stainless steel tube located downstream of the polymer injection ports. No seeding particles were premixed in the master polymer solutions. It is

difficult to ascertain how well the seeding particles mixed with the polymer solutions as the flow proceeded through the channel. However, the observation of a constant pressure gradient all along the channel and thus a constant amount of drag reduction strongly suggests that there was appreciable mixing of the water containing seed particles with the injected polymer solution. In spite of the deduction of uniform spanwise mixing in the channel there is a definite possibility that some of the more concentrated polymer threads contained no seeding particles. The maximum possible error in the measurements caused by the lack of seed particles in the polymer is discussed and estimated in the next section.

4. Results and discussion

Data from the four cases, one Newtonian and three drag reducing, are presented in this section. In all data plots, plus symbols denote the Newtonian (water) baseline case, circles represent injection of a 500 p.p.m. PEO master solution at 7.2 l/min, squares represent injection of 1000 p.p.m. PEO at 3.6 l/min, and triangles represent injection of 2000 p.p.m. PEO at 1.8 l/min. Also, where appropriate, the data in each run have been non-dimensionalized using the friction velocity of that run and the kinematic viscosity of water. The friction velocity values for each run appear in table 1. The kinematic viscosity of water was used universally because there is little difference between the viscosity of water and the viscosity of a 10 p.p.m. solution of PEO.

The mean velocity profiles for the four runs, non-dimensionalized on inner variables, appear in figure 5. The mean velocity profile for the Newtonian flow agrees quite well with the law-of-the-wall profile compiled by Coles (1953); this was shown in Willmarth *et al.* (1987). It can be seen that profiles of the three drag-reducing flows collapse onto a single curve. The deviation of the drag-reducing profiles from the Newtonian profile was extensively studied by Virk *et al.* (1967), and others. The present data exhibit a thickening of the inner region and the acceleration of the outer flow which is consistent with the earlier investigations.

The turbulence intensity profiles for the streamwise fluctuations and the fluctuations perpendicular to the wall are shown in figures 6(*a*) and 6(*b*) respectively. Figure 6(*a*) shows that the location of the maximum value of u'/u_τ is further away from the wall in the drag-reducing flows than in the Newtonian flow. In addition, the maximum value itself is greater in the drag-reducing flows. However, it should be noted that the magnitude of u' (i.e. in dimensional form) is approximately equal for the Newtonian and drag-reducing cases. This can be easily confirmed by multiplying the maximum values of u'/u_τ by the appropriate values of u_τ shown in table 1.

The fluctuations perpendicular to the wall are substantially reduced by the addition of polymers. The data in figure 6(*b*) show that the maximum value of v'/u_τ in the flow with PEO is approximately 15% less than the maximum value in water. This means that the maximum dimensional values of v' in the polymer cases are nearly 30% less than the corresponding maximum in water. Close to the wall, at a given value of y^+, the values of v'/u_τ in the drag reducing cases are as low as 50% of the Newtonian case; the dimensional values of the v-fluctuations are as low as 40% of the Newtonian case. Clearly, the effect of PEO on the fluid motions perpendicular to the wall is quite dramatic, particularly for $y^+ < 100$.

Reynolds stress profiles are presented in figure 7. The salient features of this plot are the substantial decrease in Reynolds stress upon addition of PEO, and the occurrence of negative values of Reynolds stress close to the wall in the drag-

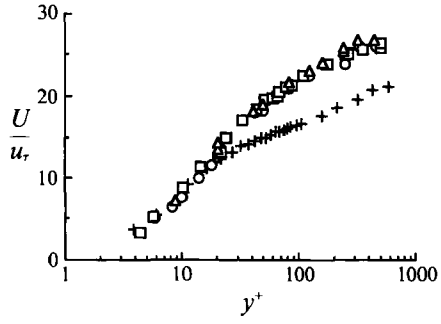

FIGURE 5. Mean velocity profiles for the four cases, non-dimensionalized on the corresponding inner variables for each case. Table 1 gives a list of symbols.

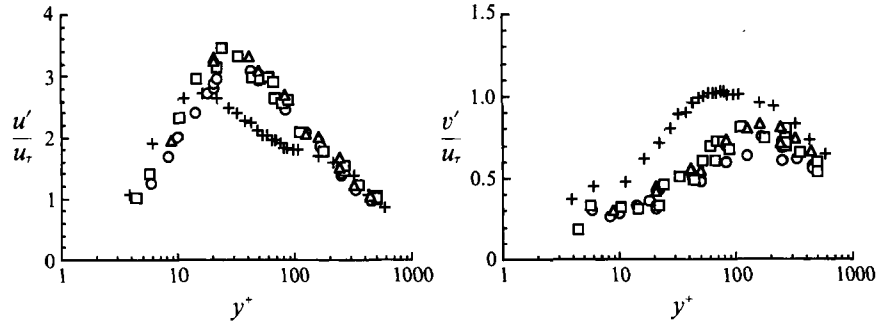

FIGURE 6. (*a*) Streamwise turbulence intensity profiles, and (*b*) wall normal turbulence intensity profiles, non-dimensionalized on inner variables, for the Newtonian and drag-reducing flows. Table 1 gives a list of symbols and friction velocity values.

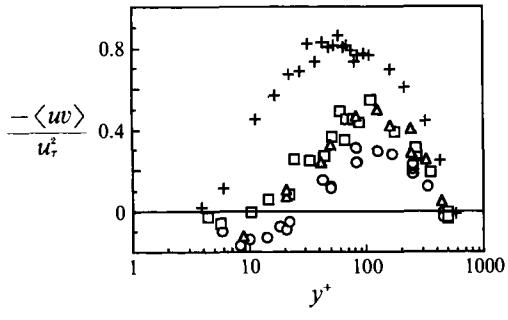

FIGURE 7. Reynolds stress profiles, non-dimensionalized on inner variables, for the Newtonian and drag-reducing flows. Table 1 gives a list of symbols and friction velocity values.

reducing cases. The decrease in Reynolds stress due to polymer addition was discussed in Willmarth *et al.* (1987). In that paper, it was pointed out that the advantage of a channel or a pipe flow is that, in a Newtonian fluid, it is possible to independently determine the Reynolds stress by subtracting the mean shear stress from the pressure gradient. The Reynolds stress for a Newtonian fluid may be found from the momentum balance, expressed as

$$-\langle uv \rangle / u_\tau^2 = [1 - y/b] - (\partial U^+ / \partial y^+). \tag{5}$$

Figure 8 shows the Reynolds stress profiles for the water and the 1000 p.p.m. PEO

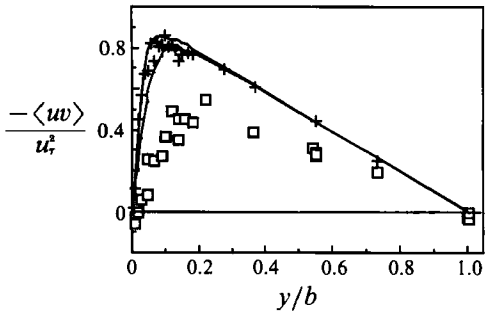

FIGURE 8. Comparison of directly measured Reynolds stress values (see table 1 for symbols) with values computed from the momentum balance equation, (5) for the Newtonian case (——) and the 1000 p.p.m. master solution case (– – –).

runs plotted versus y/b. Included in the plot are the Reynolds stress profiles computed using (5); the solid line was computed for the Newtonian case, and the dashed line for the 1000 p.p.m. injection case. Data from the 500 and 2000 p.p.m. injection cases were not included because of difficulties in accurately differentiating the mean velocity profiles to obtain $\partial U^+/\partial y^+$.

In the 500 p.p.m. case, the data were taken over a two day period using different batches of concentrated polymer with the same nominal concentration. On each day, the separation, Δy, between the points was selected so that no two adjacent points in the velocity profile were made on the same day. Because of difficulties in matching the exact conditions in the channel from one day to the next, the mean profile in the linear region was not smooth enough to accurately differentiate.

In the 2000 p.p.m. case, there was difficulty in making measurements very close to the wall. This is most likely because the mean velocity was very low ($\approx 39\%$ less than the Newtonian case at the same y^+) near the wall. Therefore, only one measurement was made in the linear region. There were not enough data to accurately compute the derivative, $\partial U^+/\partial y^+$.

There is excellent agreement between the direct measurements of Reynolds stress and the momentum balance calculations of Reynolds stress for the Newtonian flow, as shown in figure 8. This verifies that the method of measurement of velocity gradient, pressure gradient and Reynolds stress are sufficiently accurate to allow one to use the channel and measurement techniques to determine the affect of the polymer on the momentum balance and Reynolds stress. In the 1000 p.p.m. drag-reducing case, the directly measured values of Reynolds stress are positive and are approximately 60% of the corresponding values calculated from (5). For instance, at $y^+ \approx 69$, the value of non-dimensional Reynolds stress from the momentum balance equation is 0.804, while the directly measured value is only 0.450. Willmarth *et al.* (1987) concluded that this was due to the introduction of a non-Newtonian force by the polymers. That is, an additional term must be included in (5) to account for the additional forces caused by the presence of non-Newtonian polymer additives.

The existence of negative values of Reynolds stress in the range, $5 < y^+ < 25$ as seen in figure 7, was a very surprising result. If the result is correct (and it is believed that it is), it implies that the addition of polymers, at certain concentrations, leads to a unique near-wall transport process. It implies that near-wall fluid elements moving faster than the local mean speed advect away from the wall and/or fluid elements moving slower than the mean speed are advected toward the wall. In other words, for the region near the wall, the average non-Newtonian retarding force is

greater than the force attributed to the pressure gradient. Further, this non-Newtonian force has non-steady contributions which produce a mean positive correlation in the average product of the u- and v-velocity fluctuations.

A number of tests were carried out to estimate or eliminate possible sources of error in the measurements of the u-velocity, v-velocity and the Reynolds stress. First, to ensure that the negative Reynolds stress was not some type of start-up transient phenomenon, the following experiment was conducted. The LDA measuring volume was positioned at a fixed distance from the wall, and the channel flow rate was set at 360 l/min. A master solution of 500 p.p.m. PEO was then injected into the channel at a rate of 7.2 l/min. After five minutes had elapsed, one minute long data records were taken every five minutes over a period of twenty minutes. Statistics from each of the data records were computed and compared. The statistics computed from the first record were not found to be significantly different from the statistics computed from the last record. This experiment was repeated several times with the same result. It was concluded, therefore, that the negative Reynolds stress was not due to start-up transients.

Second, the possibility of probe misalignment as the cause of the negative Reynolds stress measurements was considered. This was rejected because the optical components were rigidly attached to a large optical bench. From one run to the next, the LDA was always sufficiently well aligned so that Doppler bursts were obtained without any adjustment. In order to attain the highest possible data rate with high signal-to-noise ratio, small adjustments of the LDA optics were made prior to every run. These adjustments amounted to very slight rotations of one or more of the four mirrors which direct the laser beams into the channel. These adjustments were made to bring the waists of the four laser beams into coincidence in order to maximize the simultaneous data rate. There was never a need to move any beam a distance of more than half the diameter of the measuring volume $\leqslant 25$ μm. The above alignment and adjustment procedure for the LDA system is described in more detail by Wei (1987). The fact that repeatable results satisfying the momentum equation for the flow of water in the channel, (5), were obtained with the same LDA alignment and procedures that were used for all the measurements indicates that the negative Reynolds stress measurements did not result from the LDA being out of alignment.

A third possibility, that the negative Reynolds stress measurements arose because of the non-uniform seeding of the flow, was considered. Recall that the seeding particles were injected in the settling chamber downstream of the polymer injection ports. It was hypothesized that seeding particles may not have diffused into the concentrated polymer threads. Consequently, the LDA measurements would have been obtained only when seeded Newtonian fluid was passing through the measurement volume. When a polymer thread passed through the volume, no data would have been obtained. This inability to measure velocities at certain times would affect all the velocity and Reynolds stress measurements. The largest amount of unseeded fluid injected into the flow was 2% of the channel flow rate during the injection of the 500 p.p.m. polymer solution. If the injected fluid did not contain any seed particles after mixing with the ambient seeded fluid, the data rate would be lowered by 2%. For the injection of the 1000 and 2000 p.p.m. polymer solutions at a rate of 1/100 and 1/200 of the channel flow rate the data rate would be lowered by 1% and 0.5% respectively.

To estimate the 'worst case' error caused by the omission of 2% of the data, assume that all the missing data for u and v was of the same magnitude and sign and equal to twice the maximum root-mean-square in the channel. From the values

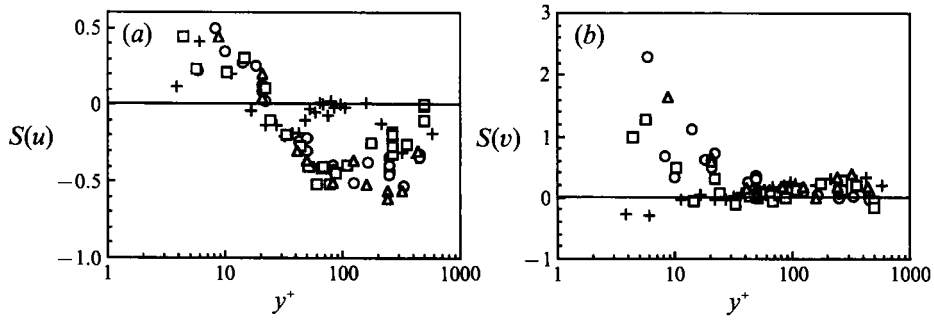

FIGURE 9. Profiles of the skewness in (*a*) the fluctuating u-signals and (*b*) the fluctuating v-signals for the four cases. Table 1 gives a list of symbols and friction velocity values.

displayed in figures 6(*a*) and 6(*b*), one would estimate that $u' \approx 7u_\tau$ and $v' \approx 1.6u_\tau$. The addition of the missing data of this magnitude to the mean-square values of u and v would increase the values of u'/u_τ and v'/u_τ by 3%.

For an estimate of the error in the Reynolds stress, assume that all the missing values had perfect correlation or anti-correlation and that both u and v were equal in magnitude to the maximum root-mean-square values displayed in figure 6. The result is that the value of $\langle uv\rangle/u_\tau^2$ would change by ± 0.07. (Note that since the correlation between u and v for a Newtonian fluid is actually only $-0.3u'v'$, this is undoubtedly an overestimate of the error.) Clearly, the estimated correction $\langle uv\rangle/u_\tau^2 = \pm 0.07$ is smaller in magnitude than the most negative Reynolds stress value shown in figure 8, $-\langle uv\rangle/u_\tau^2 \approx -0.2$. The Reynolds stress measurements close to the wall would therefore remain negative. From the above discussion and the small magnitude of the error caused by the possible non-uniformity of seed particle distribution it is concluded that the u' and v' measurements are correct and that the negative Reynolds stress values shown in figure 8 are not the result of errors in the measurements.

This is not the first paper in which negative Reynolds stress measurements have been reported. Negative values of Reynolds stress in polymer drag-reducing flows have been reported by Durst *et al.* (1985). They conducted two-component LDA measurements in a circular pipe flow using light fuel oil as the solvent. This was done primarily to match the index of refraction of the test fluid with the channel walls. However, it also had the advantage of a kinematic viscosity greater than water, which yielded relatively large viscous lengthscales.

Very close to the wall, Durst *et al.* (1985) obtained Reynolds stress measurements, non-dimensionalized by the friction velocity of the drag-reducing fluid, of approximately -0.06 in the range, $y^+ \approx 2$–3. In their discussion, they argue that u^+ is exactly equal to y^+ in the viscous sublayer. Consequently, the momentum balance equation, (5), reduces to

$$-\langle uv\rangle/u_\tau^2 = -y/b. \tag{6}$$

This will necessarily yield negative values of Reynolds stress close to the wall. They point out, however, that in their polymer case, the measured values of Reynolds stress close to the wall are more negative than would be expected from (6). (Note that the present negative Reynolds stress measurements are even more negative than those reported by Durst *et al.* 1985 for approximately the same Reynolds number. The most negative Reynolds stress measurement in figure 7 is -0.2 compared with the value -0.06 reported by Durst *et al.* 1985. Further, the most negative value in

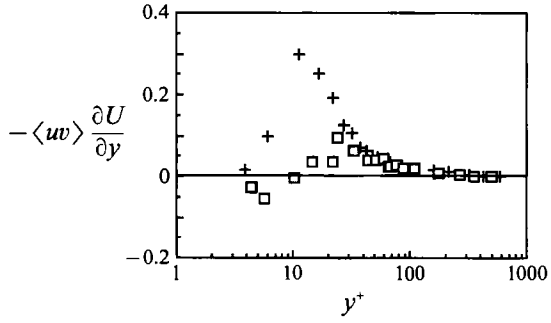

FIGURE 10. Turbulent kinetic energy production profiles for the Newtonian and drag-reducing cases. Table 1 gives a list of symbols and friction velocity values.

figure 7 occurs at $y^+ \approx 9$ as opposed to $y^+ \approx 2.5$ in Durst *et al.*) Like Willmarth *et al.* (1987), Durst *et al.* (1985) speculate on the existence of an additional non-Newtonian term in the momentum balance.

Skewness profiles for the u- and v-velocity fluctuations are shown in figures 9(*a*) and 9(*b*), respectively. It is interesting that the u-skewness profiles for water differ greatly from the polymer profiles in the range $40 \leqslant y^+ \leqslant 200$. In the v-fluctuations, the differences in the skewness profiles between the water and polymer cases are restricted to $y^+ \leqslant 20$. It is possible that these results may indicate changes in the turbulent structure due to polymer injection. However, the significance of the differences in figures 9(*a*) and 9(*b*) is not clear.

Turbulent kinetic energy production profiles for water and the 1000 p.p.m. PEO injection cases are shown in figure 10. Again, data from only one polymer case are shown because, as discussed previously, it was not possible to accurately determine the mean velocity gradient close to the wall in the other two polymer runs. Clearly, the polymers dramatically reduce the production of kinetic energy. The maximum value in the profile for 1000 p.p.m. PEO is 0.092 while the maximum value in the water profile is 0.298.

Power spectra of the data were computed at $y^+ \approx 15$, 22, 45, and 170 for the fluctuating u-, v-, and uv-signals. These spectra, shown in figures 11–14, are plotted using the format introduced by Perry & Abell (1975), and used in Wei & Willmarth (1989). The abscissa of each plot of the spectrum is the logarithm of the dimensionless frequency, $\omega^+ = \omega\nu/u_\tau^2$. The ordinate of each plot is $\Psi(\omega^+)$, which is defined so that the area beneath a semi-logarithmic plot of $\Psi(\omega^+)$ is proportional to the mean-square of the fluctuating signal, non-dimensionalized on inner variables. The relation between $\Psi(\omega^+)$ and the dimensionless power spectral density of the fluctuating signal, $\Phi(\omega^+)$, is

$$\Psi(\omega^+) = \omega^+ \Phi(\omega^+). \tag{7}$$

As in Wei & Willmarth (1989), each spectrum in figures 11–14 is an ensemble average of at least seventy individual 1024-point realizations of signal traces, reproduced at even time intervals. The traces reproduced were generated from the raw data traces at twice the average data rate and filtered with a digital Gaussian filter function. Details of the power spectrum algorithm appear in Wei (1987). For simplicity, the spectra were not plotted at frequencies greater than approximately the half-power frequency of the Gaussian filter. This was done to ensure that conclusions about drag reduction were not drawn in the frequency range where the filter was attenuating the signal; i.e. since the filter function attenuates above the half-power frequency, this truncation has no effect on the interpretation of the spectra.

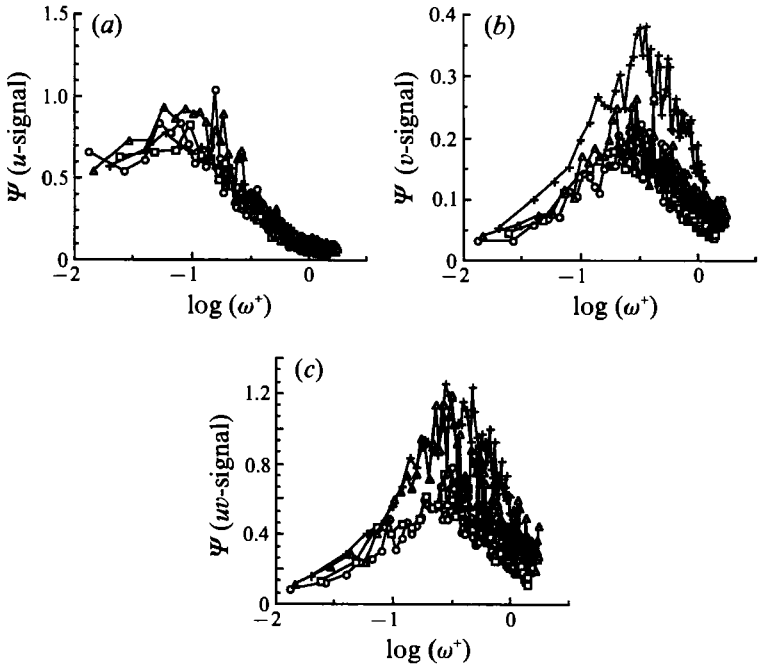

FIGURE 11. Power spectra of (*a*) the fluctuating u-velocity signals, (*b*) the fluctuating v-velocity signals, and (*c*) the fluctuating Reynolds stress signals, taken from the Newtonian flow and the three polymer cases at $y^+ \approx 170$. The spectral function, $\Psi(\omega^+)$, is defined in (7). Table 1 gives a list of symbols and friction velocity values.

Power spectra of the fluctuating u-, v-, and uv-signals recorded at $y^+ \approx 170$ appear in figures 11(*a*)–11(*c*), respectively. The u-spectra, shown in figure 11(*a*), exhibit little difference between the Newtonian case and the polymer-injection cases. Comparison with the turbulence intensity profiles in figure 6(*a*) confirms that there is little difference between the u-fluctuations in water and polymers. Very careful examination of the range $-0.5 \leqslant \log[\omega^+] \leqslant 0$ shows that the magnitudes of the water spectrum are consistently larger than the corresponding polymer values. At $y^+ \approx 170$, the differences are admittedly very slight. However, the trends become more noticeable closer to the wall. Figures 11(*b*) and 11(*c*) show that the polymers diminish the magnitudes of the v- and the uv-spectral densities in the polymer flows over the entire frequency range.

The redistribution of energy from high to low frequency in the u-fluctuations at $y^+ \approx 45$ can be clearly seen in figure 12(*a*). In the range $-0.5 \leqslant \log[\omega^+] \leqslant 0$ the magnitudes of the spectrum for the Newtonian case are noticeably larger than the spectral values in the polymer cases. However, the values of $\Psi(\omega^+)$ in the Newtonian flow for $\log[\omega^+] \leqslant -1.0$ are as much as half the values of $\Psi(\omega^+)$ in the drag-reducing flows. These results have already been observed in earlier LDA studies by Berner & Scrivener (1979) and Berman (1986). The present results are consistent with the previous works. This is an indication that the u-fluctuation data are independent of the polymer-injection geometry.

A very dramatic polymer effect appears in the spectra of the v-fluctuations at $y^+ \approx 45$, shown in figure 12(*b*). The spectral amplitudes for the three drag-reducing flows are much less than the corresponding Newtonian case over the entire frequency range. The area under the spectrum of the water data is approximately four times

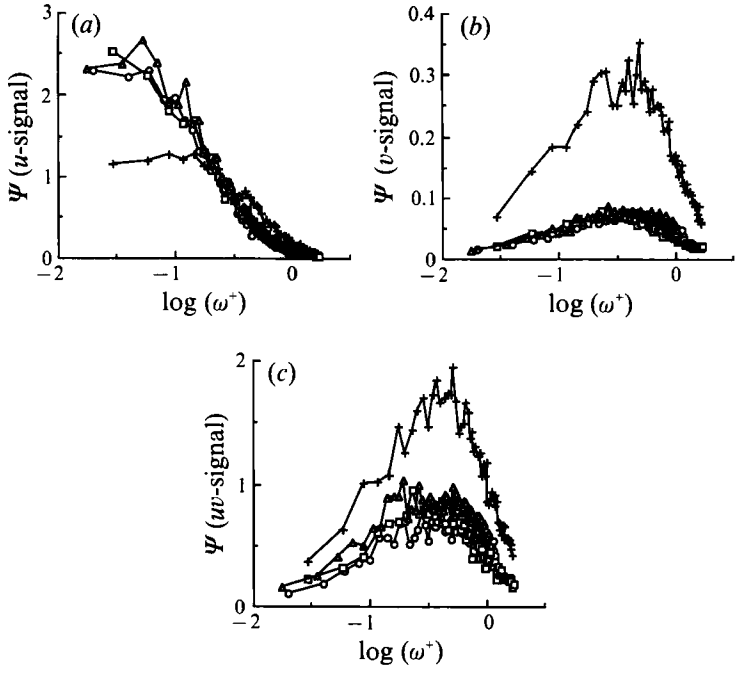

FIGURE 12. As figure 11 but at $y^+ \approx 45$.

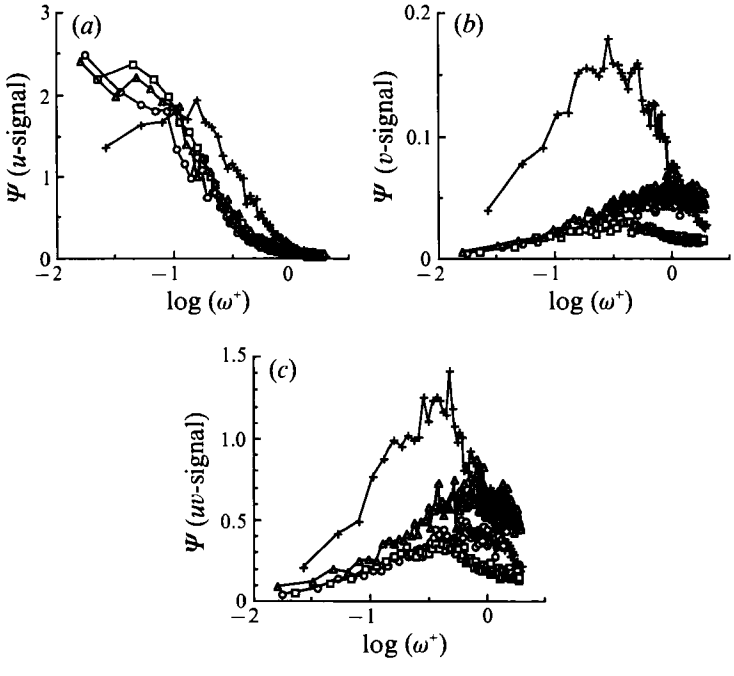

FIGURE 13. As figure 11 but at $y^+ \approx 22$.

greater than the area under any one of the polymer spectra. This is consistent with the v'/u_τ measurements shown in figure 6(*b*); the ratio of v'/u_τ for water to v'/u_τ for the polymer runs at $y^+ = 45$ is approximately two to one. The conclusion that can be drawn by comparing figures 11(*a*) and 11(*b*) with figures 12(*a*) and 12(*b*) is that the

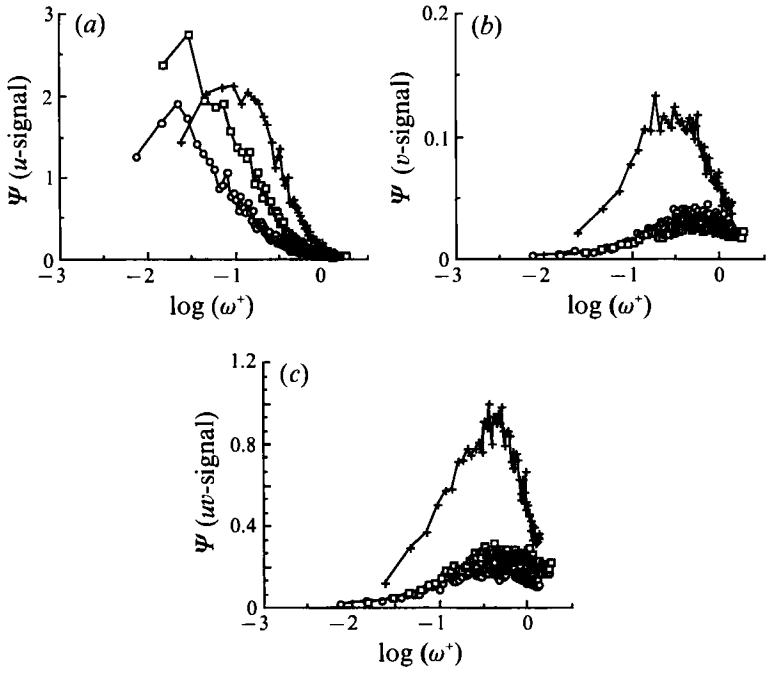

FIGURE 14. As figure 11 but at $y^+ = 15$, and only the 500 and 1000 p.p.m. master solutions.

polymers redistribute energy in the streamwise fluctuations from high frequencies to low frequencies, but the polymers severely damp the v-fluctuations over all frequencies. Further, the attenuation of the v-fluctuations has a significant effect on the Reynolds stress fluctuations. This may be seen in figure 12(*c*).

The trends of energy redistribution from high to low frequencies can be seen closer to the wall. Figures 13(*a*) and 14(*a*) show the power spectra of the u-velocity signals at $y^+ \approx 22$ and 15, respectively. Note that no data were taken at $y^+ = 15$ for the 2000 p.p.m. PEO injection case; this case is not represented in figure 14. Differences between the individual spectra for the three polymer injection cases are distinguishable in figure 13(*a*). These differences become more pronounced closer to the wall, as seen in figure 14(*a*).

It is very difficult to make any definitive qualitative statements about the effect on the flow of the different injection concentrations. Usui (1990) observed that the injection of 500 p.p.m. resulted in a rapid dispersion of polymer in the channel while the injection of 2000 p.p.m. resulted in a breakup into a large number of fine threads. One would naturally expect that there might be some difference between the different injection concentration cases. The 500 p.p.m. might be expected to more closely resemble a polymer ocean while the 2000 p.p.m. results might be more indicative of drag reduction by polymer threads. In fact, the u-spectra appearing in figure 14(*a*) clearly indicate a significant difference between the different injection conditions. Further, comparison of percentage drag reduction as a function of injection conditions, shown in table 1, indicate that injecting a higher-concentration solution at a lower flow rate yields greater drag reduction than the converse. This issue requires further investigation using a wider range of injection concentrations and flow rates.

Finally, figures 13(*b*) and 14(*b*) show the spectra of the v-velocity fluctuations which remain suppressed by the polymers close to the wall. The suppression of the

fluctuations normal to the wall is consistent with the reduction in Reynolds stress exhibited in the polymer-addition cases. Spectra of the time-dependent Reynolds stress signals appear in figures 13(*c*) and 14(*c*) for $y^+ \approx 22$ and 15, respectively, and strongly resemble the spectra for the v-velocity signals.

5. Conclusions

High-resolution, two-component LDA measurements were made in a fully developed turbulent channel flow with and without the injection of polyethylene oxide. Three different 'master' solution concentrations were tested at a 'homogeneous' concentration of 10 p.p.m. The Reynolds number for all tests was approximately 12000. Data rates were sufficiently high so that it was possible to compute power spectra of not only the fluctuating u-velocity but the fluctuating v-velocity and Reynolds stress signals as well. Critical examination of the results led to the following conclusions:

(i) Polymers dramatically attenuate the v-velocity fluctuations throughout the channel over the entire frequency range.

(ii) For certain polymer concentrations negative Reynolds stress with a magnitude of the order of $\langle uv \rangle / u_\tau^2 \approx 0.2$ was measured in the region near the wall.

(iii) Polymers dramatically attenuate the Reynolds stress fluctuations throughout the channel over the entire frequency range.

(iv) There is a marked difference in the u-velocity spectra and the Reynolds stress in the region near the wall when the same amount of polymer in a solution of three different concentrations is injected into the flow before it enters the channel.

(v) The differences in the u-velocity spectra and Reynolds stress close to the wall are consistent with the observations of Berman (1990), Usui (1990), and others that the breakup of 500 p.p.m. injected polymer is significantly different from the breakup of 2000 p.p.m. injected polymer.

We gratefully acknowledge A. Sagar of MIT for many helpful discussions on polymer chemistry including a supply of salient titles from the polymer chemistry literature. We also acknowledge Professor N. S. Berman of Arizona State University for his insight into polymer drag reduction. The experimental work was made possible through the support of The Office of Naval Research Contract No. N00014 84 K 0414 P00002 monitored by Dr M. M. Reischman during the 3 year experimental phase of this investigation. The first author received summer support from the David Taylor Research Center through a US Navy-ASEE Summer Faculty Fellowship.

REFERENCES

Achia, B. U. & Thompson, D. W. 1977 Structure of the turbulent boundary in drag-reducing pipe flow. *J. Fluid Mech.* **81**, 439.

Berman, N. S. 1977 Flow time scales and drag reduction. *Phys. Fluids* **20**, S168.

Berman, N. S. 1986 Velocity fluctuations in non-homogeneous drag reduction. *Chem. Engng Commun.* **42**, 37.

Berman, N. S. 1990 Large eddies and polymer strings. In *Structure of Turbulence and Drag Reduction* (ed. A. Gyr), p. 275. Springer.

Berner, C. & Scrivener, O. 1979 Drag reduction and structure of turbulence in dilute polymer solutions. In *Viscous Flow Drag Reduction* (ed. G. R. Hough). Progress in Astronautics and Aeronautics, vol. 72, p. 290. *AIAA*.

BEWERSDORFF, H. W. 1984 Heterogene Widerstandsverminderung bei turbulenten Rohrströmungen. *Rheol. Acta* **23**, 522.

BRADSHAW, P. 1965 The effect of wind tunnel screens on nominally two-dimensional boundary layers. *J. Fluid Mech.* **22**, 679.

COLES, D. 1953 Measurements in the boundary layer of a smooth flat plate in supersonic flow; Part I. The problem of the turbulent boundary layer. *JPL/Cal Tech Rep.* 20–69.

DONOHUE, G. L., TIEDERMAN, W. G. & REISCHMAN, M. M. 1972 Flow visualization of the near-wall region in a drag-reducing channel flow. *J. Fluid Mech.* **56**, 559.

DURST, F., KECK, T. & KLEINE, R. 1985 Turbulence quantities and Reynolds stress in pipe flow of polymer solutions, *Proc. 1st Intl Conf. on Laser Anemometry – Advances and Applications*, p. 31. BHRA.

GORDON, R. J. 1970 Mechanism for turbulent drag reduction in dilute polymer solutions. *Nature* **227**, 599.

HINCH, E. J. 1977 Mechanical models of dilute polymer solutions in strong flows. *Phys. Fluids* **20**, S22.

KLINE, S. J., REYNOLDS, W. C., SCHRAUB, F. A. & RUNSTADTLER, P. W. 1967 The structure of turbulent boundary layers. *J. Fluid Mech.* **30**, 741.

LUCHIK, T. S. & TIEDERMAN, W. G. 1988 Turbulent structure in low-concentration drag-reducing channel flows. *J. Fluid Mech.* **190**, 241.

LUMLEY, J. L. 1969 Drag reduction by additives. *Ann. Rev. Fluid Mech.* **1**, 367.

MCCOMB, W. D. & RABIE, L. H. 1982 Local drag reduction due to injection of polymer solutions into turbulent flow in a pipe. *AICHE J.* **28**, 547.

MCCORMICK, C. L., HESTER, R. D., MORGAN, S. E. & SAFIEDDINE, A. M. 1990*a* Water-soluble copolymers. 30. Effects of molecular structure on drag reduction efficiency. *Macromol.* **23**, 2124.

MCCORMICK, C. L., HESTER, R. D., MORGAN, S. E. & SAFIEDDINE, A. M. 1990*b* Water-soluble copolymers. 31. Effects of molecular parameters, solvation, and polymer associations on drag reduction performance, *Macromol.* **23**, 2132.

PERRY, A. E. & ABELL, C. J. 1975 Scaling laws for pipe flow turbulence. *J. Fluid Mech.* **67**, 257.

RABIN, Y. & ZIELINSKA, B. J. A. 1989 Scale-dependent enhancement and damping of vorticity disturbances by polymers in elongational flow. *Phys. Rev. Lett.* **63**, 512.

REISCHMAN, M. M. & TIEDERMAN, W. G. 1975 Laser–Doppler anemometer measurements in drag-reducing channel flows. *J. Fluid Mech.* **70**, 369.

RUDD, M. J. 1972 Velocity measurements made with a laser dopplermeter on the turbulent pipe flow of a dilute polymer solution. *J. Fluid Mech.* **51**, 673.

STENBERG, L. G., LAGERSTEDT, T., SEHLÉN, O. & LINDGREN, E. R. 1977 Mechanical mixing of polymer additive in turbulent drag reduction. *Phys. Fluids* **20**, 858.

TIEDERMAN, W. G., LUCHIK, T. S. & BOGARD, D. G. 1985 Wall-layer structure and drag reduction. *J. Fluid Mech.* **156**, 419.

USUI, H. 1990 Drag reduction caused by the injection of a polymer solution into a pipe flow. In *Structure of Turbulence and Drag Reduction* (ed. A. Gyr). Springer.

VIRK, P. S., MERRILL, E. W., MICKLEY, H. S., SMITH, K. A. & MOLLO-CHRISTENSEN, E. L. 1967 The Toms phenomenon: turbulent pipe flow of dilute polymer solutions. *J. Fluid Mech.* **30**, 305.

WEI, T. 1987 Reynolds number effects on the small scale structure of a turbulent channel flow, Ph.D. thesis, The University of Michigan.

WEI, T. & WILLMARTH, W. W. 1989 Reynolds number effects on the structure of a turbulent channel flow. *J. Fluid Mech.* **204**, 57.

WILLMARTH, W. W., WEI, T. & LEE, C. O. 1987 Laser anemometer measurements of Reynolds stress in a turbulent channel flow with drag reducing polymer additives. *Phys. Fluids* **30**, 933.

ZAKIN, J. L. & HUNSTON, D. L. 1980 Effect of polymer molecular variables on drag reduction. *J. Macromol. Sci. Phys.* B**18**, 795.